Experimental Study of Noise Temperature and Conversion Loss of SIS Junction Mixers

J. C. Macfarlane,[A] *L. B. Whitbourn*[A,B] *and R. A. Batchelor*[C]

[A] Division of Applied Physics, CSIRO, P.O. Box 218, Lindfield, N.S.W. 2070.
[B] Present address: Division of Mineral Physics and Mineralogy, CSIRO,
P.O. Box 218, Lindfield, N.S.W. 2070.
[C] Division of Radiophysics, CSIRO, P.O. Box 76, Epping, N.S.W. 2121.

Abstract

Experiments on the performance of superconductor–insulator–superconductor (SIS) tunnel junctions as heterodyne mixers at 40 GHz are reported. The techniques developed for the fabrication of multi-junction SIS series arrays differ from, and are considerably simpler than, other methods described in the literature. Results are reported on mixer noise temperature, conversion loss, saturation, local oscillator power levels and mixer dynamic range. Factors affecting the mixer's conversion performance are identified and comparisons are made with other reported results. It is concluded that mixer performance in the present experiments is limited by imperfect impedance matching at the signal frequency, due to relatively large values of parasitic capacitance in the junctions. Future work is aimed at both reducing the junction capacitance and redesigning the mixer mount to give improved r.f. matching.

1. Introduction

A structure consisting of two superconducting films separated by a thin insulating layer has strongly nonlinear characteristics quite apart from the Josephson effects. The nonlinear properties of interest are due to the onset of a quasiparticle (i.e. single-electron) tunnelling current (Giaever and Megerle 1961) at voltages corresponding to the edge of the superconducting energy gap. This characteristic indicates that superconductor–insulator–superconductor (SIS) devices should have interesting properties as classical detectors or mixers. Tucker (1979) has shown that non-classical behaviour is expected to occur when the photon energy hf/e of the incoming radiation is sufficiently large on the voltage scale of the nonlinearity to switch the junction from a non-conducting to a conducting state. He further showed (Tucker 1980) that for a mixer in which all sidebands other than the signal, image and intermediate frequency are short-circuited, conversion gain was possible. This contrasts with the case of a classical mixer with similar restrictions (Torrey and Whitmer 1948) which always exhibits conversion loss. The possibility of achieving conversion gain, together with the expectation that SIS junctions would have inherently low-noise tunnelling properties, stimulated a great deal of experimental research into SIS mixers.

Conversion gain has now been achieved by a number of research groups; for example, D'Addario (1984), McGrath *et al.* (1981) and Kerr *et al.* (1981). Tucker

and Feldman (1985) gave an up-to-date review of the subject. A major incentive for the work is to lower the detection threshold of radio-astronomy receivers, although other applications utilizing the outstanding receiver sensitivity will almost certainly follow. The present study was initiated in 1982 jointly by the Divisions of Applied Physics and Radiophysics of the CSIRO, with the following aims:

  (i)   to develop techniques for the production of SIS multi-junction mixers;
  (ii)   to set up cryogenic and microwave equipment for the precise measurement of the conversion performance and noise temperature of SIS mixer arrays;
  (iii) to make quantitative comparisons of the measurements with the reported results of other groups;
  (iv)   to identify aspects of the initial experiments where improvements should be made, with the eventual aim of developing an SIS mixer for radio-astronomy applications.
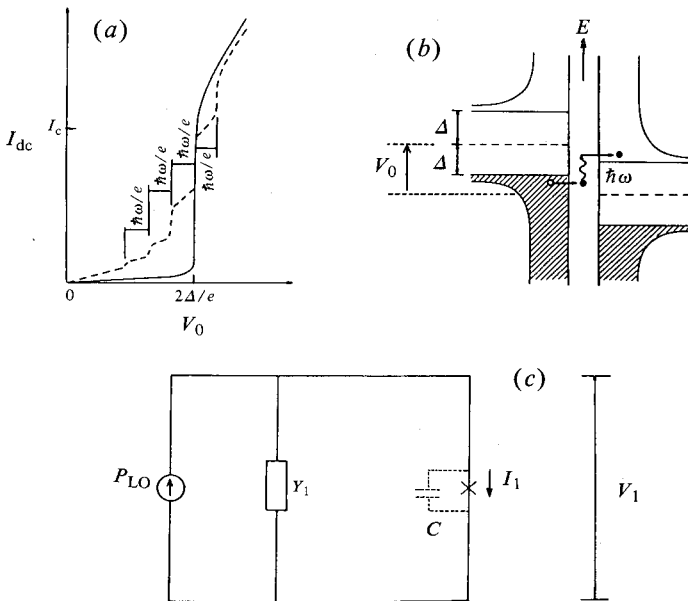

Fig. 1. Diagrams showing (*a*) quasiparticle *I–V* characteristics for an SIS junction; (*b*) energy-level diagram for the SIS tunnelling structure; (*c*) equivalent circuit diagram for an SIS junction coupled to the local oscillator and waveguide; Y_1 represents the complex source admittance presented to the junction.

2. Theory

(a) Quasiparticle Tunnelling

We assume two superconducting films having identical energy gaps are separated by a thin insulating layer (e.g. an oxide film about 2 nm thick). The d.c. *I–V* characteristic of such a junction due to quasiparticle tunnelling is represented in Fig. 1*a* by the solid

curve. The sharp onset of current occurs when the applied potential corresponds to the energy-gap voltage $2\Delta/e$. In the presence of high-frequency radiation a d.c. current flows below the energy-gap voltage due to photon-assisted tunnelling as illustrated in Fig. 1 b. The I–V curve then takes on the shape of the broken curve (Fig. 1 a). The detailed form of this 'pumped' curve is given by the expression

$$I_{\mathrm{p}} = \sum_{n=-\infty}^{\infty} J_n^2(\alpha)\, I_0(V_0 + nhf/e), \qquad \alpha = eV_1/hf \qquad (1)$$

(Tien and Gordon 1963), where I_0 is the 'unpumped' curve, V_0 is the d.c. voltage, V_1 is the peak r.f. voltage across the junction and J_n is the nth order Bessel function. A schematic circuit is shown in Fig. 1 c, where the junction (represented by a cross) is coupled to the local oscillator (LO). The theoretical expression (1) can be fitted to experimental I–V curves to deduce values for α, and hence the r.f. voltage V_1.

The peak r.f. current I_1 flowing through the junction is in general out of phase with the applied voltage, due to quantum reactance terms. It is given by

$$I_1 = F(\alpha), \qquad (2)$$

where $F(\alpha)$ is a complex quantity (Feldman 1982) which can be computed numerically once α is known.

The junction capacitance C, as discussed below, may have a major effect on the performance of the mixer. The net capacitance can be reduced, however, by employing a series array of N junctions. Provided the overall length of the array is negligible compared with the wavelength, the theory derived for a single junction remains applicable, with relevant impedances and voltages being multiplied where appropriate by N (Feldman and Rudner 1983).

(b) Heterodyne Mixing with SIS Junctions

The theory of mixing in the quantum-mechanical regime has been extensively discussed by Tucker and Feldman (1985). Only those arguments and definitions that are relevant to the present work will be summarized here.

Mixer conversion loss. Conversion loss is defined for a single-sideband mixer under conditions of ideal r.f. and i.f. matching as

$$L = P_{\mathrm{s}}/P_{\mathrm{if}}, \qquad (3)$$

where P_{s} is the signal power available from the source and P_{if} is the power delivered to the i.f. load. The SIS junction is inherently a broad-band device but, owing to the large parasitic capacitance of the junction, it is difficult to achieve broad-band matching with conventional mixer structures. Matching is therefore optimized in practice for one sideband, and so all results reported here will be treated as single-sideband measurements. The prediction by Tucker (1980) of available mixer gain implies that in optimum conditions, and for equal image and signal terminations, $L < 1$.

Mixer noise temperature. The noise temperature T_m of a mixer is defined as the temperature at which Johnson noise in a matched input resistor would give rise to the measured amount of i.f. output noise power from the mixer; for example, if the measured output noise power is P' (W) in a bandwidth B (Hz), then

$$T_m = LP'/kB. \tag{4}$$

A lower limit to T_m is set by the uncertainty principle at (Tucker and Feldman 1985)

$$T_m > hf/k,$$

i.e. approximately $1 \cdot 9$ K at 40 GHz. In practice, excess noise will usually be observed due to random fluctuations in the tunnelling current. An authoritative treatment of the quantum limits on noise has been given by Caves (1982).

Mixer dynamic range. The useful dynamic range of an SIS mixer can be estimated by assuming that saturation will occur when the amplitude of the i.f. voltage swing V_{if} exceeds some appreciable fraction of the 'photon step' voltage hf/e. (For an array of N junctions, the corresponding quantity is Nhf/e.) Tucker and Feldman (1985) proposed that 'gain compression' of 1 dB will occur when $V_{if} > 0 \cdot 2 Nhf/e$. For a load resistance R_L and conversion loss L, this implies the onset of saturation at an input power level of

$$P(\text{sat.}) = (0 \cdot 2 Nhf/e)^2 L/2R_L. \tag{5}$$

The dynamic range of the mixer can then be expressed as

$$P(\text{sat.})/P(\text{min.}) = (0 \cdot 2 Nhf/e)^2 L/2R_L \, kT_m \, B, \tag{6}$$

where the input noise power $kT_m B$ is arbitrarily taken to be the minimum detectable signal.

3. Experimental Techniques

(a) Junction Manufacture

The SIS devices were prepared at the National Measurement Laboratory (NML) of the Division of Applied Physics by vacuum deposition of lead or lead alloy films through a mask onto fused silica substrates. The mask consisted of a fine electroformed mesh (15 μm wires at 35 μm spacing) stretched over a 10 μm wide slit. The substrate (dimensions $20 \times 1 \cdot 3 \times 0 \cdot 12$ mm) was mounted above the slit on a micrometer-driven carriage so that it could be translated longitudinally relative to the mesh with a precision of ± 2 μm. A string of base electrodes, 10×35 μm in size, was first formed by evaporating a PbIn alloy through the mesh. The alloy contained 27 at.% indium. The base electrodes were allowed to oxidize in air for 60–90 min at 40°C. The substrate was then translated by 25 μm and a second evaporation of pure Pb formed a second set of identical electrodes which overlapped the first set.
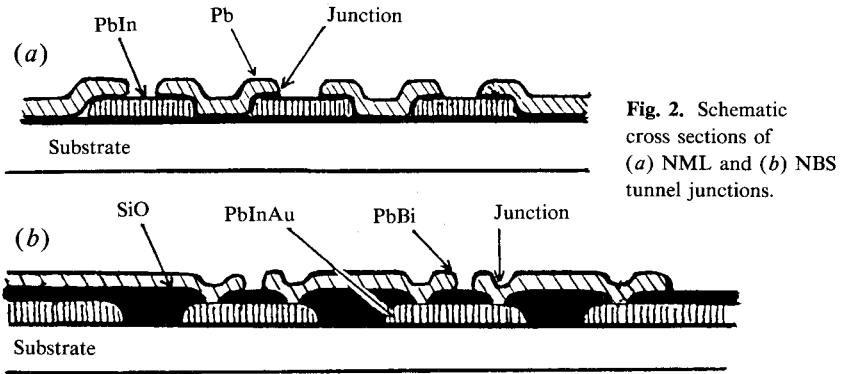
Fig. 2. Schematic cross sections of (*a*) NML and (*b*) NBS tunnel junctions.

Fig. 3. Surface analysis of PbIn film. The four curves represent the removal of successive layers from 2 to 60 monolayers.
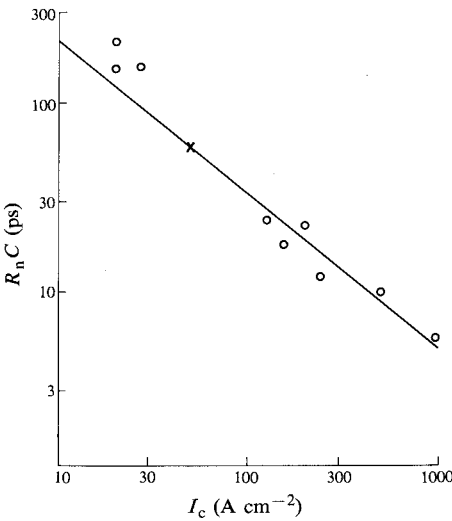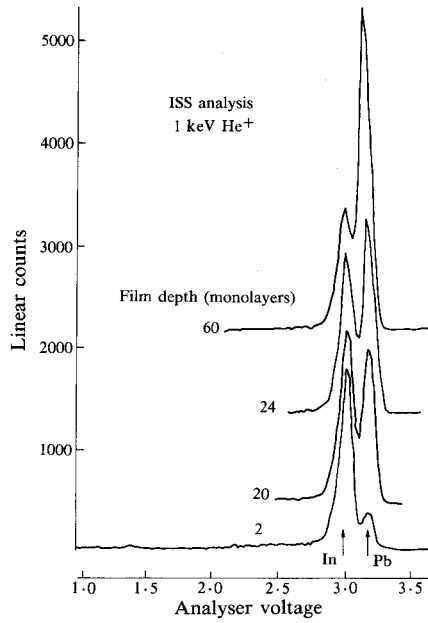
Fig. 4. Relationship between tunnelling current density I_c and time constant $R_n C$ for nine NML arrays (circles) and one NBS array (cross).

A series connected array of PbIn–oxide–Pb junctions of area $10 \times 10 \ \mu m^2$ was thus formed. Two stripline conductors incorporating low-pass filters were then deposited to connect the junction array to contacts at the ends of the substrate.

An SIS device made at the US National Bureau of Standards (NBS) (Shen *et al.* 1980) was also used in the present measurements. It differed from the NML junctions in the following respects: the junction area was $20 \ \mu m^2$; the junctions were defined by 'windows' in a thick insulating layer covering the base electrodes; the base electrodes were of a PbInAu alloy; the counter-electrodes were of PbBi; and the substrate was a silicon wafer. Details of both types of junction are shown schematically in Fig. 2.

(b) General Properties of the Tunnel Junctions

The thin oxide layer separating the superconducting electrodes is crucial in determining the properties of the device. We have shown by surface analysis (inelastic scattering spectroscopy, ISS) that the surface of the base electrodes consists predominantly of In to a depth of about 20 monolayers (Fig. 3). This supports the assertion of Havemann *et al.* (1978) that the barrier is composed of In_2O_3. We have deduced the capacitance of our junctions from the results of Magerlein (1981) which relate to this type of oxide barrier.

The superconducting energy gap 2Δ of the two electrodes determines the onset voltage V_g for tunnelling according to the formula

$$e V_g = \Delta_{Pb} + \Delta_{PbIn} .$$

At the normal operating temperature of 1·8–2 K

$$\Delta_{Pb} = 1 \cdot 35 \ meV , \qquad \Delta_{PbIn} = 1 \cdot 28 \ meV ,$$

(Adler *et al.* 1967) giving

$$V_g(1 \cdot 8 \ K) = 2 \cdot 63 \ mV .$$

It can be shown (e.g. Gasparovich *et al.* 1966) that the corresponding value at 4·2 K is

$$V_g(4 \cdot 2 \ K) = 2 \cdot 34 \ mV .$$

We have measured V_g for many of our PbIn–oxide–Pb junctions singly and in series arrays and we obtained

$$V_g(1 \cdot 8 \ K) = 2 \cdot 65 \pm 0 \cdot 1 \ mV , \qquad V_g(4 \cdot 2 \ K) = 2 \cdot 40 \pm 0 \cdot 1 \ mV ,$$

in satisfactory agreement with the published data.

The time constant of a tunnel junction array is given by $R_n C$, where R_n is the resistance corresponding to the linear part of the *I–V* curve (well above the energy gap) and C is the capacitance of the array. Harris and Hamilton (1978) demonstrated a direct correlation between the response time and the critical current density I_c as represented by the straight line in Fig. 4. The open circles (representing 9 NML arrays) and the cross (1 NBS array) are clearly consistent with the data of Harris and Hamilton. It might seem that an SIS device designed to operate at 40 GHz should

have a response time of the order of 25 ps or less (i.e. to ensure that $2\pi f RC < 1$). However, several experimental studies (see e.g. Pan *et al.* 1983) have shown that $2\pi f RC$ may be as large as six provided the array's capacitance can be adequately 'tuned out' at the signal frequency by adjustment of the mixer mount controls.

Fig. 5. Photograph of lower half of the SIS mixer mount.

10 mm
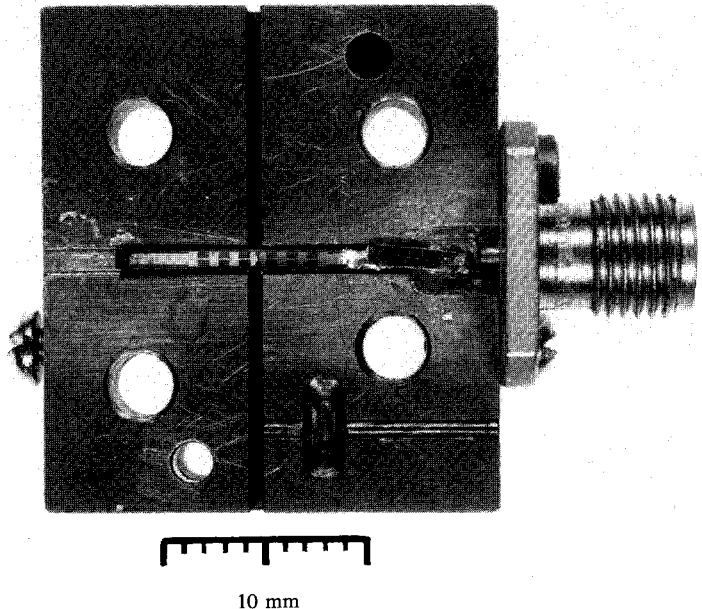
(c) Conversion Performance and Noise Temperature Measurement Techniques

The SIS devices were mounted in a mixer block (Fig. 5) across a reduced-height waveguide. An adjustable tuning stub and a sliding back-short were provided to allow some degree of adjustment in the matching of the complex impedance of the array to the waveguide. A miniature coaxial connector provided d.c. and i.f. connections to one end of the array, the other end of the array being grounded to the waveguide structure. Some 20 SIS devices were produced, and detailed measurements were carried out on about half of them. It was found that the arrays operated repeatably over a period of some weeks if they were kept at liquid nitrogen temperatures; however, exposure to room air for several days caused degradation to set in. The NBS device, which incorporated the materials and manufacturing techniques developed by IBM for their Josephson computer research, was much more durable and survived months at room temperature without any serious change in its characteristics.

A schematic layout of the experiment is shown in Fig. 6. A calibrated signal at a frequency f_s in the range 36–42 GHz was applied via an adjustable precision attenuator and a 20 dB attenuator at 2 K. The local oscillator at frequency f_{LO} ($f_s - f_{LO} = 1 \cdot 5$ GHz) was coupled to the same stainless steel waveguide. The d.c. connections were decoupled from the i.f. line by means of a bias tee in the helium bath. The i.f. output at $1 \cdot 5$ GHz was fed to a radiometer/reflectometer test set, similar to the one referred to by Weinreb and Kerr (1973) which was adjusted to read directly in K by reference to matched loads at 77 and 295 K (ports A and B). The bandwidth of the radiometer was 100 MHz.

The mixer's conversion loss, equivalent input noise temperature and i.f. mismatch were deduced from the measured i.f. port temperature under three conditions: (i) no external signal applied (T_1), (ii) a calibrated 40 GHz signal applied at the r.f. port (T_2), (iii) a calibrated noise signal applied at the i.f. port (T_3). Corrections for the finite losses and noise due to the i.f. coaxial cable (GC) were derived from measurements on the auxiliary cables installed in the cryostat (D, EF). These measurements were carried out at regular intervals during an experimental run so that systematic effects due to the changing liquid helium level, for example, could be taken into account. The r.f. losses in the waveguide were measured in a separate experiment.
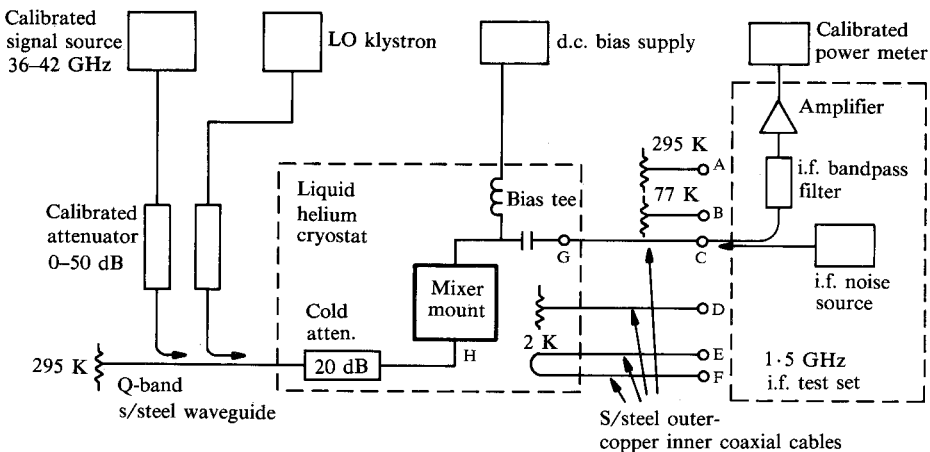

Fig. 6.   Schematic diagram of the measuring equipment.

The single-sideband loss L and noise temperature T_m of the mixer are given by

$$L = \Delta T_{\text{sig}} \beta (1 - |\Gamma_{\text{if}}|^2)(T_2 - T_1)^{-1}, \tag{7}$$

$$T_m = \Delta T_{\text{sig}}\{T_1 - T_6 - \beta|\Gamma_{\text{if}}|^2(T_5 + \beta T_A)\}(T_2 - T_1)^{-1} - T_{\text{in}}, \tag{8}$$

where T_1, T_2 and T_3 are as defined above; ΔT_{sig} is the equivalent temperature of the signal referred to the mixer input; $|\Gamma_{\text{if}}|^2$ is the i.f. reflection coefficient; β is the transmittance of the i.f. cable (~ 0.85); T_5 and T_6 are the thermal noise radiating temperatures out of the lossy i.f. cable at its cold and hot ends respectively (T_5 is generally slightly less than T_6 in the present experiment and both are of the order of 20 K, as derived from measurements on auxiliary cables D, EF); T_{in} is the room temperature radiation referred to the input of the mixer; T_A is the actual room temperature. We note that ΔT_{sig} and T_{in} take into account the effects of waveguide losses and the cold attenuator.

The calculation of L and T_m together with the corrections as outlined above are based on unpublished notes by A. R. Kerr. Experimental errors in loss measurements, which arise mainly from uncertainties in the losses occurring in the waveguide components, the cold attenuator and the i.f. output connections, are estimated to be ± 1 dB. Noise temperature measurements are subject to uncertainties in all of the temperatures appearing in (8), and are also affected by the relatively large values of conversion loss found in the present experiments. It is estimated that the noise temperatures reported here are subject to an experimental error of ± 20 K, except where otherwise stated.

(d) Impedance Matching

The expressions (3) and (4) in Section 2 for loss and noise temperature assume ideal coupling exists between the SIS array and (*a*) the input waveguide structure, and (*b*) the i.f. output load. In practice, these conditions are seldom achieved. In the present work the input matching was optimized by adjusting the back-short and the stub tuner until an apparent maximum in i.f. output was reached. This technique allowed a wide range of SIS devices to be used but, where the capacitive reactance of the array is smaller than the tunnelling resistance R_n, this technique becomes unreliable. The i.f. output impedance was not adjustable, but the measurement procedure allowed the i.f. reflection coefficient to be calculated. Thus the reported results have been corrected for i.f. mismatch but not for any residual mismatch in the r.f. mixer input.
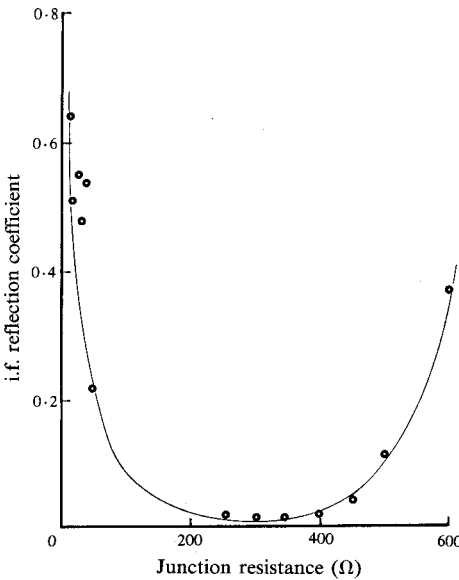

Fig. 7. Dependence of the i.f. reflection coefficient on the resistance of the junctions.

4. Results

(a) The i.f. Reflection Coefficient

The conversion loss and i.f. reflection coefficient were measured for SIS arrays ranging in d.c. tunnelling resistance from 12 to 600 Ω. Although the mixer's dynamic resistance at $1 \cdot 5$ GHz is not necessarily identical to R_n, a systematic correlation was

obtained as shown in Fig. 7. It is clear that junction arrays having R_n in the range 150–450 Ω are well matched to the i.f. output line. It is estimated, from inspection of the junction's pumped tunnelling characteristics, that the dynamic resistance at the i.f. operating point is in most cases about $0 \cdot 5 R_n$.
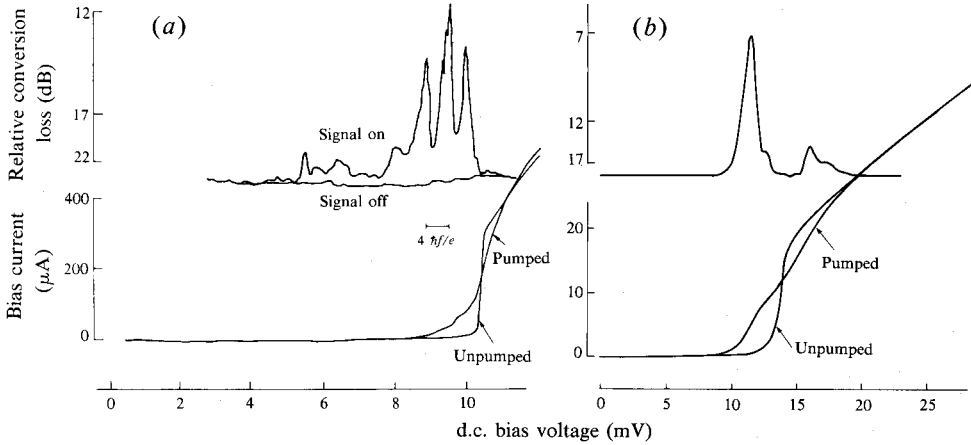

Fig. 8. Typical *I–V* characteristics and mixer conversion curves for (*a*) a 4-junction NML array (LO power, 2 μW) and (*b*) a 5-junction NBS array (LO power, 8 μW).

(b) Measurements of Mixer Conversion Performance

General features of the mixer's conversion performance are shown in Fig. 8*a* for a 4-junction NML array. Deflections in the pumped *I–V* curve corresponding to photon-assisted tunnelling steps are clearly visible. The three dominant maxima in the i.f. output occur at bias voltages corresponding to one, two and three photon steps below the energy gap.

The best performance for an NML array was achieved with a 10-junction device having a tunnelling resistance of 500 Ω and a capacitance of $0 \cdot 3$ pF. It gave a conversion loss of 10 dB and a noise temperature of 12 ± 10 K at $41 \cdot 5$ GHz.

Corresponding results for the NBS 5-junction array are shown in Fig. 8*b*. The nonlinearity in the unpumped curve is less sharp than in the case of the NML array, and there are no well-resolved photon steps in the pumped curve. Only one broad conversion peak could be resolved in the i.f. output, but its position changed with local oscillator power, suggesting the presence of several broad, overlapping conversion maxima centred on neighbouring photon steps. This array, which had a tunnelling resistance of 600 Ω and a capacitance of $0 \cdot 15$ pF, gave a conversion loss of $5 \cdot 2$ dB, the best result so far achieved with the present mount. We attribute the performance of this array to its relatively low capacitance. The measured noise temperature was 15 ± 13 K.

(c) Conversion Performance against Number of Junctions

Although the performance of SIS mixer arrays has been extensively studied (e.g. Rudner *et al.* 1981) no previous attempt has been reported of varying in a controlled way the number of junctions actually operating as mixers in a given series array.

Fig. 9. Variation of mixer noise temperature, i.f. reflection coefficient and conversion loss with number of junctions operating.
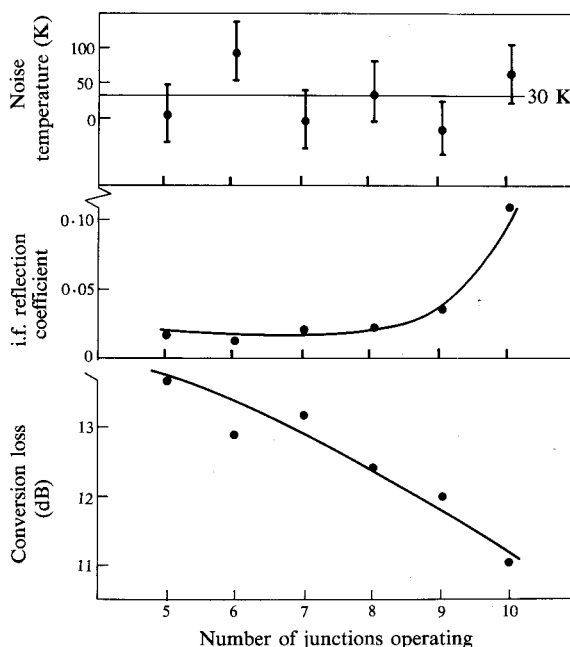
It is possible to do this by making use of the fact that for small values of magnetic field and LO power levels the quasiparticle tunnelling current may be a multi-valued function of d.c. bias voltage, successive branches of the I–V curve corresponding to $n = 1, 2, 3, ..., N$ junctions in series. The d.c. bias voltage and the LO power can be carefully adjusted so that n ($<N$) junctions are operating as quasiparticle tunnel junctions, the remainder ($N - n$) being in a superconducting (d.c. Josephson) state. The latter can be regarded as superconducting shorts in series with the mixer, but a detailed treatment would take into account the parametric inductance due to the Josephson current. In practice it is difficult to achieve stable mixer operation for $n < N$, but useful data were obtained for $n = 5$–10 in the case of a 10-junction array, as shown in Fig. 9. It can be seen that (a) the conversion efficiency improved due to the reduction in capacitance with increasing n; (b) the i.f. reflection coefficient was at a minimum for six junctions; and (c) the mixer noise temperature was independent of the number of junctions within the experimental uncertainty. The noise temperatures, as calculated by means of equation (8), depend on algebraic differences between relatively large, almost equal, contributions which are each subject to experimental uncertainties. The individual points are thus scattered about the mean, and in some cases have apparent negative values. It is emphasized that this apparently non-physical result arises from the experimental difficulties in making precise noise temperature measurements in the presence of large conversion loss. Much more accurate determinations of SIS mixer noise have been reported by McGrath *et al.* (1985).

(d) Conversion Performance against Capacitance of the Array

An attempt was made to correlate the best measured conversion efficiency of each array with its known physical properties, for example, tunnelling resistance R_n, capacitance C, time constant $R_n C$ and current density. No correlation was found

apart from the one illustrated in Fig. 10 where the conversion loss is plotted against capacitance for 12 NML arrays and one NBS array. The results of Räisänen *et al.* (1985), also shown, were obtained using single junction mixers made at NBS, some of which incorporated a stripline inductor which was designed to resonate out the junction capacitance at the 36 GHz signal frequency. Thus the upper limit of their experimental results can be taken as an independent benchmark indicating the best performance to be expected from junctions of the type described. In our present measurements it was always difficult to achieve optimum r.f. matching, due partly to imperfections in the design and mechanical adjustments of the tuning elements, and partly (we believe) to the finite length of the arrays. The overall effect of imperfect matching has been crudely estimated by assuming that some constant fraction $\Delta C/C$ of the capacitance remains as a shunt susceptance across the waveguide at the mixer input. We can then estimate how the performance of the mixer should vary with C, assuming the equivalent circuit driving the capacitively shunted junction is a constant-current source. The result is the smooth curve in Fig. 10, which has been fitted to the experimental data at one point only (the point 0·5 pF, 12·9 dB), with $\Delta C/C = 0·28$. It is interesting to note that the extrapolation of the curve to zero capacitance indicates that a modest amount of conversion gain (about 0·1 dB) should then be realized.
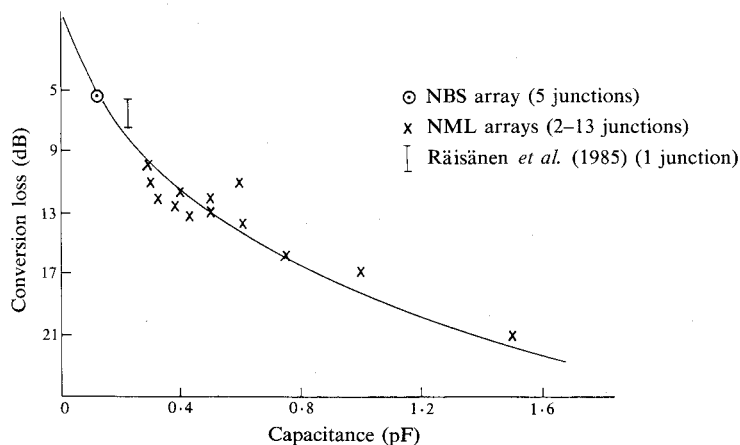

Fig. 10.   Relationship between conversion loss and capacitance of the array.

(e) Interpretation of the Pumped I–V Curves

As described in Section 2*a* the detailed shape of the *I–V* curves under the action of the local oscillator can provide information about the r.f. voltage amplitude and the r.f. currents flowing in the junction array. In particular, by using a computer to find values of α which make expression (1) a good fit to the experimental data, the corresponding values of r.f. voltage amplitude $V_1 = \alpha hf/e$ can be calculated. In general α is expected to vary with d.c. voltage bias because of the changing dynamic resistance along the *I–V* curve. The experimental points (Fig. 11, circles) were obtained for a 10-junction array having $R_n = 60\ \Omega$ and $C = 0·4$ pF. Evidently the single value $\alpha = 5·0$ gives a reasonable fit at all bias voltages (solid curve). This suggests that the r.f. voltage amplitude is insensitive to changes in the tunnelling
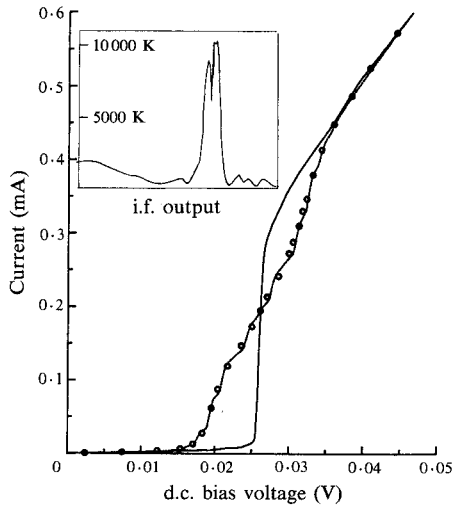
Fig. 11. Comparison of the theoretical pumped I–V curve with experimental points (circles) for a 10-junction array. The solid curve was computed for $\alpha = 5 \cdot 0$. The inset is discussed in the text.

resistance which, for the array under discussion, ranged from about 20 to 200 Ω. The uncompensated capacitance of the array would be expected to reduce the effect of changes in the tunnelling resistance, as observed.

It is of interest to estimate the LO power dissipated in the mixer array at the operating point (Fig. 11, inset) where the i.f. conversion is at a maximum. Computing the best fit at this point gives $\alpha = 4 \cdot 59$; hence

$$V_1 = 7 \cdot 59 \text{ mV}$$

and, from equation (2),

$$I_1 = (103 + 18) \, \mu\text{A} \,.$$

The dissipation is then

$$0 \cdot 5 \, V_1 \, \text{Re}(I_1) = 0 \cdot 4 \, \mu\text{W} \,.$$

The applied LO power was $4 \cdot 8 \, \mu\text{W}$, implying that the coupling coefficient at the LO frequency was only 8%. This is consistent with the large r.f. mismatch inferred from the conversion measurements.

(f) Mixer Dynamic Range

The response of two mixer arrays to input power levels ranging from 5 pW to 5 nW is shown in Fig. 12. Both devices are linear over most of the range but the onset of saturation can be seen. The departure from linearity amounts to 1 dB at $0 \cdot 4$ nW for the NBS 5-junction array and at 3 nW for the NML 6-junction array. A major advantage of multi-junction arrays over single-junction mixers is that the saturation power level (equation 5) increases as N^2. Equation (5) gives saturation power levels for these arrays of $0 \cdot 51$ and $2 \cdot 31$ nW respectively, in good agreement with the measured values. The measured noise temperatures of the two arrays were 8 K (NBS) and 20 K (NML). Equation (6) then allows us to estimate the dynamic range of these SIS mixers:

$$3 \cdot 6 \times 10^4 \quad \text{(NBS 5-junction array)}, \qquad 1 \cdot 1 \times 10^5 \quad \text{(NML 6-junction array)} \,.$$

Fig. 12. Mixer output as a function of signal strength showing onset of saturation for the NBS 5-junction array (circles) and the NML 6-junction array (crosses).
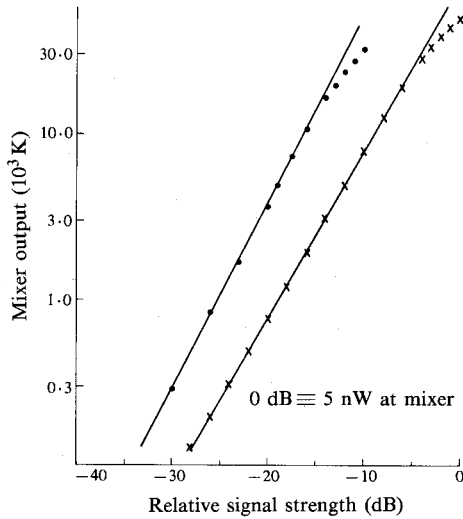
5. Conclusions

The SIS mixers based on PbIn–oxide–Pb multi-junction arrays were made and tested at 35–42 GHz. The general properties of the junctions such as current density, capacitance/unit area, energy gap, 'sharpness' and nature of the oxide layer, were shown to be consistent with existing data in the literature. Mixer noise temperatures were typically in the range 30 ± 20 K, in broad agreement with other reported results at 40 GHz, while conversion loss figures were greater than anticipated. The effects of i.f. mismatch, number of junctions in the array and capacitance were elucidated.

Computer programs were developed to enable comparisons to be made between theory and the experimental pumped curves, and to estimate the LO voltage, current and power dissipation in the junctions. Typically, less than 1 μW absorbed LO power was sufficient to achieve optimum mixer performance.

The results indicated that the measured conversion performance was adversely affected by the excessive capacitance of the arrays. The adjustments of sliding back-short and tuning stub were in principle capable of tuning out the junction capacitance but it was concluded that for the relatively large junctions used (100 μm^2 in area) residual unmatched capacitance remained a problem. This conclusion was reinforced when an SIS array made by the US National Bureau of Standards with smaller junctions (20 μm^2) installed in our mixer block gave significantly better performance. The measurements carried out on the NBS array enabled us to compare our results with other recent work on similar junctions and indicated that conversion gain might be expected to occur if the junction capacitance could be effectively tuned out at the signal frequency.

Measurements of the onset of saturation in our SIS mixers were in agreement with theoretical estimates, and confirmed the useful dynamic range expected for multi-junction arrays.

In the immediate future our intention is to make use of a mixer mount of improved design which should provide greater control over the r.f. input matching. It is also planned to develop arrays of much smaller capacitance using 'edge-aligned' junctions (Macfarlane and Banasiak 1985) and to achieve more durable devices by using niobium instead of lead-alloy films.

Acknowledgments

References

Adler, J. G., Jackson, J. E., and Will, T. A. (1967). *Phys. Rev. Lett.* A **24**, 407.
Caves, C. M. (1982). *Phys. Rev.* D **26**, 1817.
D'Addario, L. (1984). *Int. J. Infrared Millimeter Waves* **5**, 1419.
Feldman, M. J. (1982). *J. Appl. Phys.* **53**, 584.
Feldman, M. J., and Rudner, S. (1983). *Rev. Infrared Millimeter Waves* **1**, 47.
Gasparovich, R. F., Taylor, B. N., and Eck, R. E. (1966). *Solid State Commun.* **4**, 59.
Giaever, I., and Megerle, K. (1961). *Phys. Rev.* **122**, 1101.
Harris, R. E., and Hamilton, C. A. (1978). 'Future Trends in Superconductive Electronics' (Eds B. S. Deaver *et al.*), p. 448 (American Inst. Phys.: New York).
Havemann, R. H., Hamilton, C. A., and Harris, R. E. (1978). *J. Vac. Sci. Technol.* **15**, 392.
Kerr, A. R., Pan, S.-K., Feldman, M. J., and Davidson, A. (1981). *Physica* B **108**, 1369.
Macfarlane, J. C., and Banasiak, I. (1985). *Appl. Surf. Sci.* **22/23**, 1027.
McGrath, W. R., Räisänen, A. V., Richards, P. L., Harris, R. E., and Lloyd, F. L. (1985). *IEEE Trans. Mag.* **21**, 212.
McGrath, W. R., Richards, P. L., Smith, A. D., van Kempen, H., Batchelor, R. A., Prober, D. E., and Santhanam, P. (1981). *Appl. Phys. Lett.* **39**, 655.
Magerlein, J. H. (1981). *IEEE Trans. Mag.* **17**, 286.
Pan, S. J., Feldman, M. J., and Kerr, A. R. (1983). *Appl. Phys. Lett.* **43**, 786.
Räisänen, A. V., McGrath, W. R., Richards, P. L., and Lloyd, F. L. (1985). Broad-band r.f. match to a mm-wave SIS quasiparticle mixer. *IEEE Trans. Microwave Theory Tech.* **MTT-33**, 1495.
Rudner, S., Feldman, M. J., Kollberg, E., and Claeson, T. (1981). *J. Appl. Phys.* **52**, 6366.
Shen, T. M., Richards, P. L., Harris, R. E., and Lloyd, F. L. (1980). *Appl. Phys. Lett.* **36**, 777.
Tien, P. K., and Gordon, J. P. (1963). *Phys. Rev.* **129**, 647.
Torrey, H. C., and Whitmer, C. A. (1948). Crystal rectifiers. MIT Radiation Lab. Series No. 15 (McGraw–Hill: New York).
Tucker, J. R. (1979). *IEEE J. Quantum Electron.* QE **15**, 1234.
Tucker, J. R. (1980). *Appl. Phys. Lett.* **36**, 477.
Tucker, J. R., and Feldman, M. J. (1985). *Rev. Mod. Phys.* **57**, 1055.
Weinreb, S., and Kerr, A. R. (1973). *IEEE J. Solid State Circuits* SC **8**, 58.